AD-A218 469 DOCUMENTATION PAGE

Form Approved
OMB No. 0704-0188

1a. REPORT SECURITY CLASSIFICATION: Unclassified	1b. RESTRICTIVE MARKINGS
2a. SECURITY CLASSIFICATION AUTHORITY	3. DISTRIBUTION/AVAILABILITY OF REPORT: Approved for public release; distribution is unlimited.
2b. DECLASSIFICATION/DOWNGRADING SCHEDULE	
4. PERFORMING ORGANIZATION REPORT NUMBER(S)	5. MONITORING ORGANIZATION REPORT NUMBER(S): AFOSR-TR- 90-0181
6a. NAME OF PERFORMING ORGANIZATION: Stanford University; 6b. OFFICE SYMBOL (If applicable)	7a. NAME OF MONITORING ORGANIZATION: AFOSR/NA
6c. ADDRESS (City, State, and ZIP Code): Department of Mechanical Engineering, Stanford University, Stanford, CA 94305	7b. ADDRESS (City, State, and ZIP Code): Building 410, Bolling AFB DC 20332-6448
8a. NAME OF FUNDING/SPONSORING ORGANIZATION: AFOSR/NA; 8b. OFFICE SYMBOL (If applicable): NA	9. PROCUREMENT INSTRUMENT IDENTIFICATION NUMBER: AFOSR 84-0373
8c. ADDRESS (City, State, and ZIP Code): Building 410, Bolling AFB DC 20332-6448	10. SOURCE OF FUNDING NUMBERS: PROGRAM ELEMENT NO. 61102F; PROJECT NO. 2308; TASK NO. A2; WORK UNIT ACCESSION NO.

11. TITLE (Include Security Classification)

(U) Topology of Three-Dimensional, Variable Density Flows

12. PERSONAL AUTHOR(S)

B. Cantwell, G. Lewis, J. Chen

13a. TYPE OF REPORT	13b. TIME COVERED	14. DATE OF REPORT (Year, Month, Day)	15. PAGE COUNT
Reprint	FROM 9/1/84 TO 6/30/89	December 1989	6 pages

16. SUPPLEMENTARY NOTATION

17. COSATI CODES		
FIELD	GROUP	SUB-GROUP
21	01	
21	02	

18. SUBJECT TERMS (Continue on reverse if necessary and identify by block number)
Combustion, Reacting Flows, Turbulent Mixing, Diagnostics, Particle Tracking, Flow Topology

19. ABSTRACT (Continue on reverse if necessary and identify by block number)

This paper is concerned with the interpretation of unsteady, variable-density flow fields. The topology of the flow is determined by finding critical points and identifying the character of local solution trajectories. The time evolution of the flow is studied by following the paths of the critical points in the three-dimensional space of invariants of the local deformation tensor. The methodology can be applied to any smooth vector field and its associated gradient tensor including the vorticity and pressure gradient fields. This approach provides a framework for describing the geometry of complex flow patterns. Concisely summarizing that geometry in the space of invariants of the local gradient tensor may be a useful way of gaining insight into time-dependent processes described by large computational data bases. Applications to the description of a flickering diffusion flame and a compressible wake are discussed.

20. DISTRIBUTION/AVAILABILITY OF ABSTRACT: ☒ UNCLASSIFIED/UNLIMITED ☒ SAME AS RPT. ☐ DTIC USERS	21 ABSTRACT SECURITY CLASSIFICATION: Unclassified
22a. NAME OF RESPONSIBLE INDIVIDUAL: Julian M Tishkoff	22b TELEPHONE (Include Area Code): (202) 767-4935; 22c. OFFICE SYMBOL: AFOSR/NA

Paper prepared for
the 10th Australasian Fluid Mechanics Conference, Melbourne Australia December 1989

Topology of Three-dimensional, Variable Density Flows

Brian Cantwell, Gregory Lewis
Stanford University, Stanford, CA 94305

Jacqueline Chen
Sandia National Laboratories, Livermore, CA 94550

ABSTRACT

This paper is concerned with the interpretation of unsteady, variable - density flow fields. The topology of the flow is determined by finding critical points and identifying the character of local solution trajectories. The time evolution of the flow is studied by following the paths of the critical points in the three-dimensional space of invariants of the local deformation tensor. The methodology can be applied to any smooth vector field and its associated gradient tensor including the vorticity and pressure gradient fields. This approach provides a framework for describing the geometry of complex flow patterns. Concisely summarizing that geometry in the space of invariants of the local gradient tensor may be a useful way of gaining insight into time - dependent processes described by large volumes of data. Applications to the description of a flickering diffusion flame and a compressible wake will be discussed.

1. INTRODUCTION

Advances in computation and measurement techniques have led to a rapid increase in our ability to generate vast quantities of unsteady flow field data. A wide variety of flows are being computed or measured experimentally using an almost equally wide variety of methods. Direct numerical simulation at moderate Reynolds number is now an established tool for the study of turbulent flows even in the presence of complicating conditions such as heat release, compressibility, buoyancy and the like. However, despite this success, a true understanding of turbulence still eludes us and there is a growing realization that, to an important degree, the future usefullness of simulation for problem solving and for gaining new understanding will rest on our ability to synthesize complex flow information. The key to this will be to find systematic methods for reducing three-dimensional flow patterns to basic elements in order to identify, summarize and relate significant features of the data.

Topological methods are useful in the description of fields. They focus attention on the problem of connecting vortex structures together to complete the flow field and they provide a description of complex flow patterns in terms of a limited set of elementary patterns which can occur near critical points in the field. Recently Chong, Perry and Cantwell (1988) have carried out a classification of the various types of elementary three-dimensional flow patterns which can occur near critical points in compressible and incompressible flow. If the vector field of interest is linearized about the the critical point $x^c = (x^c_1, x^c_2, x^c_3)$ the result is

$$\frac{dx_i}{ds} = A_{ij}\,(x_j - x^c_j) \qquad (1)$$

and the local trajectories of the vector field are given by the solution $x(s; x^c)$. If the flow field is unsteady the pattern at an instant is considered and s is a parameter along the instantaneous field lines. If the flow pattern is steady and A_{ij} is the velocity deformation tensor, $\partial u_i / \partial x_j$, then s is equivalent to the time in the motion of a fluid particle along a streamline.

Let the deformation tensor be broken up into a symmetric and an antisymmetric part, $\partial u_i / \partial x_j = S_{ij} + R_{ij}$, where $S_{ij} = (\partial u_i/\partial x_j + \partial u_j/\partial x_i)/2$ and $R_{ij} = (\partial u_i / \partial x_j - \partial u_j / \partial x_i)/2$ are the strain and rotation tensors respectively. The eigenvalues of A_{ij} satisfy the characteristic equation

$$\lambda^3 + P\lambda^2 + Q\lambda + R = 0 \qquad (2)$$

where the matrix invariants are:

$$P = -(a_{11} + a_{22} + a_{33}) = -\text{trace}\,[A] = -S_{ii} \qquad (3)$$

$$Q = \begin{vmatrix} a_{11} & a_{12} \\ a_{21} & a_{22} \end{vmatrix} + \begin{vmatrix} a_{11} & a_{13} \\ a_{31} & a_{33} \end{vmatrix} + \begin{vmatrix} a_{22} & a_{23} \\ a_{32} & a_{33} \end{vmatrix}$$

$$= \frac{1}{2}\left[P^2 - \text{trace}[A^2]\right] = \frac{1}{2}\left[P^2 - S_{ij}S_{ji} - R_{ij}R_{ji}\right] \qquad (4)$$

and

$$R = -\begin{vmatrix} a_{11} & a_{12} & a_{13} \\ a_{21} & a_{22} & a_{23} \\ a_{31} & a_{32} & a_{33} \end{vmatrix} = -\det[A]$$

$$= (1/3)\left(-P^3 + 3PQ - \text{trace}[A^3]\right)$$

$$= (1/3)\left(-P^3 + 3PQ - S_{ij}S_{jk}S_{ki} - 3R_{ij}R_{jk}S_{ki}\right) \qquad (5)$$

It can be shown that, in the P-Q-R space of matrix invariants, there exists a surface which divides real solutions from complex solutions. This surface is given by

$$27R^2 + (4P^3 - 18PQ)R + (4Q^3 - P^2Q^2) = 0 \qquad (6)$$

The topology of a given vector field is identified as follows.

i) Locate the critical points of the field and evaluate the nine partial derivatives of the field variables at each point.

ii) Evaluate P, Q and R at the critical points. The local topology is determined by the position of a critical point with respect to the surface (6). A detailed discussion of the properties of this surface is given in Chong, Perry and Cantwell (1988) along with a guide to the various possible elementary flow patterns which can occur in different domains.

iii) The time evolution of the flow topology is followed by repeating steps (i) and (ii) at each instant and plotting the resulting path of each critical point in (P, Q, R) space. Bifurcations in the flow topology occur when critical points first appear, merge, split or change type as their trajectory crosses the surface (6) or other boundaries between topologically distinct domains.

This scheme has several attractive features for concisely summarizing the behavior of flow fields. In an incompressible flow the first invariant of the velocity gradient tensor is zero and therefore the trajectories of the critical points are restricted by continuity to lie in the plane of the second and third invariants. In this case the complete topological history of a three-dimensional flow can be represented in a plane. The vorticity vector field is interesting because the first invariant of the vorticity gradient tensor, $\partial \omega_i / \partial x_j$, is zero for both compressible and incompressible flow. The pressure gradient vector field is interesting because the gradient tensor of this field, $\partial p / \partial x_i \partial x_j$, always has real eigenvalues with orthogonal eigenvectors.

In the present paper, data for a flickering diffusion flame and a compressible wake are interpreted using this approach. These efforts are at a very early stage and we are still at the point of trying to ask the right questions.

2. UNSTEADY DIFFUSION FLAME

Lewis, Cantwell, Vandsburger and Bowman (1988) used particle tracking to measure instantaneous velocity fields in an unsteady methane - air diffusion flame subject to a classical, periodic, flickering instability. These measurements were used to picture the topology of a flame undergoing breakup. Figure 1 shows a typical processed image of the vector field data measured in these experiments. More recently complete vector fields were measured by Lewis (1989) over the first 25 diameters above the fuel jet exit. There exists in this flow a relatively unambiguous means of choosing the most appropriate frame of reference. As the flickering instability develops a confined region of high strain rate develops on the axis approximately six jet diameters downstream of the fuel jet exit. Although there are significant buoyancy-induced accelerations inside the flame the high strain rate disturbance moves vertically upward at a nearly constant speed and is used to define an appropriate frame of reference. The velocity field in Figure 1 is plotted with respect to an observer moving with this disturbance.

Figure 1 also indicates various salient features of the flame including the image produced by soot radiation which appears as a heavy black envelope surrounding the fuel-rich core of the flame. Several critical points are also indicated; a lower saddle, which in this figure is indicated at the top near the flame tip, an outer ring vortex beneath the flame surrounding the flame neck and an upper saddle located at the base of the flame. The reason for the apparent ambiguity in naming the saddles has to do with the periodicity of the flame and the fact that they are really part of the same flow structure which tends to be located between adjacent rolled-up flames.

This is made clear in Figure 2 which depicts a sequence of frames showing the complete evolution of flame topology during the flickering cycle over the first 25 diameters of the flow. The dashed line in this figure corresponds to the soot envelope seen in Figure 1. The necking down and eventual pinching off of this envelope leads to the breakup of the flame. This figure indicates that the flickering instability in a diffusion flame involves a distinct birth, growth and decay cycle of a cellular vortex-ring-like structure. This structure originates at a point approximately six diameters downstream of the jet exit and is associated with the high strain rate disturbance described earlier. As the vortex ring develops the soot envelope is distorted into a tent-like shape with the flow near the upper saddle tending to stretch the envelope outward, rolling it up into the center, while the movement of air toward the axis near the lower saddle tends to push the envelope inward eventually causing the flame to pinch off. The relatively rapid growth of the vortex and concomitant increase in its apparant mass act to offset the acceleration by buoyancy helping to explain the observed constant convection velocity of the vortex ring.

The flicker instability is driven by, but not soley dependent upon, buoyancy and some understanding of the basic mechanism can be gained by examining velocity data very near the jet exit. The release of heat in a cylindrical sheet surrounding the jet exit creates a hollow plume which rises under the action of buoyancy. The acceleration of fluid on the jet axis begins slowly but becomes stronger as heat is conducted to the jet centerline. As the flow accelerates the flame sheet contracts, further increasing the rate of heat transfer to the centerline, further accelerating the flow, further increasing the heat transfer and so forth. Also contributing to the acceleration and pinch-off on the centerline is the diffusion of momentum radially inward due to the opposite signed vorticity contained in the flame generated plume. This opposite signed vorticity is produced within a couple of diameters of the jet exit and persists for a considerable distance downstream. As the flame sheet pinches off this vorticity accumulates near the upper saddle giving it a peculiar re-entrant appearance imparting a heart shape to the overall structure as seen in Figures 1 and 2. The vortex structure retains this heart-shape until the vorticity at the upper saddle is convected outward and downward into the center terminating the flickering cycle.

Figure 3 depicts the evolution of the flow in P, Q, R coordinates where the velocity derivatives have been normalized by the jet exit velocity and jet diameter. To simplify the discussion each invariant is plotted on a separate set of axes. The first invariant, P, is the negative of the flow divergence and is related to heating and cooling of fluid in the neighborhood of the critical point. A feeling for the relative magnitude of P can be gained by examining Figure 3(d) which indicates the magnitude of the strain and vorticity at the critical points. The normalized vorticity at the center attains a maximum value of 5 compared to normalized values of P at the saddles which lie between -2 and 2. In other words typical levels of flow divergence are comparable to typical levels of vorticity and can be expected to play a significant role in the flow dynamics. The flow divergence at the center remains very close to zero over most of the cycle. The birth of the vortex structure occurs at Phase 2 with the first appearance of critical points in this frame of reference. The value of P at the lower saddle tends to remain

A-1

negative indicating a slowly decreasing density probably related to heating at the saddle through conduction. The upper saddle seems to begin with relatively rapid cooling possibly associated with the convection along the axis of relatively cooler core fluid as the soot envelope is pushed outward.

The second invariant, Q, is shown in Figure 3 (b). The centers (really a line surrounding the jet axis) show a slowly increasing value of Q, indicating more intense rotation, until flame pinch-off occurs after which Q falls almost to zero. An examination of the time evolution of Q and R (Figure 3 c) clearly reveals the birth, growth and decay cycle referred to earlier. Flame pinch-off is a very well defined event with all of the invariants of the critical points tending rapidly to zero after the event. Another feature which is revealed is that the upper and lower saddle points have a very different character. Figure 3 (d) indicates that the magnitude of the axial extensive strain at the lower saddle is considerably smaller than the magnitude of the axial compressive strain at the upper saddle. This difference becomes even more apparent when R, which is proportional to the cube of the strain rates, is plotted in Figure 3 (c). This figure depicts a rapid build-up and then fall-off of R at the upper saddle while R at the center and lower saddle remains close to zero throughout the cycle. Although we have just begun to study the topology of flames in (P, Q, R) space these initial results suggest that the invariants of the deformation tensor can serve as a sensitive indicator of flame dynamics.

3. COMPRESSIBLE PLANE WAKE

Efforts are presently under way to determine the topology of the velocity, vorticity and pressure gradient vector fields in the compressible wake computations of Chen, Cantwell and Mansour (1989)[1] and Chen, Mansour and Cantwell (1989). This work is at a very early stage and at the writing of this paper the results are both preliminary and quite incomplete. Very recently we have found that in the early stages of instability the 2-D wake topology is similar to the topology of two mixing layers separated by an alleyway. As the disturbances grow a bifurcation occurs wherein the saddles on opposite sides of the wake become connected. These results are discussed in Chen, Cantwell and Mansour (1989)[2] presented at this conference. In the present paper I would like to make some remarks about the 3-D vorticity and pressure gradient fields. All the results will pertain to one case in which the initial free-stream Mach number is one and velocity defect Mach number is 0.692. The wake Reynolds number is 300.

Figure 4 shows instantaneous streamlines in the wake a short time after the onset of the motion. The lines are produced by integrating particle tracks with the velocity field frozen. The initial positions of the particles are chosen to lie in two planes; one at the midpoint and one at the side boundary of the domain. The initial field consists of a 3-D oblique wave superimposed on a 2-D wave chosen to coincide with the most amplified mode. In the absence of the 3 - D disturbance the centers are joined in the spanwise direction by a degenerate line. Adding the 3-D disturbance creates a connection in the spanwise direction and the centers become stretching and contracting foci with flow from the centerline moving outward toward the boundary.

Figure 5 shows two views of vortex lines in the wake at a late stage in the three-dimensional development (dimensionless time t = 64). The vorticity, which was initially only slightly perturbed from being aligned in the spanwise direction, has formed a series of highly flattened vortex loops or discs inclined to the direction of flow. One of the observations of this work has been that all of the flow structure observed in incompressible wakes is also seen in the compressible case but delayed in time due to the lower amplification rates. In the case presented here, the critical points first appear when the wake defect Mach number is well below one. Although there are significant temperature and density variations throughout the field, density changes due to heat conduction occur relatively slowly. As a consequence P is nearly zero and the critical points can be depicted in the Q-R plane.

Each of the vortex discs contains a center and a saddle in the vorticity vector field and the computational domain contains six such structures. From symmetry considerations the critical points associated with each vortex disc should have the same values of P, Q, and R. However because the data is numerically determined on a grid there is some uncertainty in determining derivatives at the critical points and as a result there is some scatter in the location of the critical points in this plane. Moreover the vorticity vector field tends to be highly degenerate in the sense that there are extended regions where the vorticity and its first derivatives are close to zero. As the Reynolds number is increased, the more extensive these flat regions become. Figure 6 shows the values of Q and R at t = 64 determined at the six centers and at one saddle. Symbols for two of the centers overlay each other and the symbol for one of the centers is very close to the origin reflecting the basically degenerate nature of the field. The remaining saddles are located in regions where the vorticity is very flat and if they exist at all they cannot be distinguished by our present method of data interpolation. The center point occurs near the apparant center of the vortex disc and the saddle lies outside of the disc and between adjacent vortex loops where the direction of the vorticity vector reverses to align with the neighboring structure in the streamwise direction. The interesting thing is that, for the critical points which can be distinguished, the value of R is very nearly zero implying that the center is indeed a center and not a focus and that the saddle is locally two-dimensional. How can these features be so two-dimensional when the basic flow is so obviously three-dimensional ? Chong, Perry and Cantwell (1989) discuss the possible existence of skewed two dimensional vector fields and we see such an example here in the wake. With a bit of effort a SLINKY toy can be stretched, bent and skewed into a configuration which resembles the vortex lines in Figure 5.

Two examples of the pressure gradient vector field at t = 59 are shown in Figure 7. The pressure gradient field in two planes aligned with the flow direction is shown. In Figure 7 (a) the plane is chosen to pass through the maximum in streamwise vorticity ; ie. through the side of the vortex disc. In Figure 7 (b) the plane is chosen to pass through the minimum in streamwise vorticity; ie. diametrically through the center of the disc. The pressure gradient patterns in both cases are similar except for the strength which is somewhat larger in case (a). As expected the critical points all have real eigenvalues and, if they exist, orthogonal eigenvectors. To the extent that viscous

transport of momentum can be neglected the pressure gradient vectors can be thought of as the negative of the acceleration field. In this variable the flow structure is seen to consist of a sequence of unstable nodes near the vortex centers separated by saddle points which lie between the vortices. The problem of degeneracy also arises in connection with this field which goes to zero in the free stream. However within the body of the flow critical points are easy to distinguish and the pressure gradient field appears to be a good indicator of important features of the flow field.

4. CONCLUDING REMARKS

Each of the fields considered has advantages and disadvantages for flow interpretation and a great deal of work beyond these fledgling efforts needs to be done in order to determine the variable or set of variables which will work best in a given situation. The topology of the velocity vector field is relatively easy to distinguish but depends on the frame of reference. The topology of the vorticity vector field is independent of the observer and can be displayed in the Q-R plane. But at high Reynolds number the vorticity field tends to be degenerate and full of holes requiring a higher order approach which is likely to be difficult to apply in practice. In this instance traditional critical point concepts lose their usefullness and need to be replaced by general mathematical methods for dealing with higher order field topology. The pressure gradient field is independent of the motion of a non-accelerating observer and has easily identifiable critical points with orthogonal eigenvectors. Usually the pressure gradient decays outside the vortical region leading to a degeneracy problem in identifying critical points near the edges of the flow. However the degeneracy of the pressure, which decays algebraically, is not as serious as that of the vorticity which decays exponentially and, in practice, it should be possible to model the external pressure field using analytic functions.

ACKNOWLEDGEMENT

Support of the AFOSR under grant AF - 84 - 0373 the Department of Energy under contract DE - ACC4 - 76DP00789 and NASA Ames Research Center is gratefully acknowledged.

REFERENCES

CHEN, J. CANTWELL, B. and MANSOUR, N. 1989[1] The effect of Mach number on the stability of a plane supersonic wake. AIAA paper 89 - 0285 presented at the 27th Aerospace Sciences Meeting, Reno, Nevada.

CHEN, J. CANTWELL, B. and MANSOUR, N. 1989[2] The topology and vorticity dynamics of a three-dimensional plane compressible wake. In *Proceedings of the 10th Australasian Fluid Mechanics Conference*, Melbourne, Australia December 11-15, 1989.

CHEN, J., MANSOUR, N. and CANTWELL, B. 1989 Direct Numerical Simulations of Transition in a Compressible Wake. In *Proceedings of The Seventh Symposium on Turbulent Shear Flows*, August, Stanford University.

CHONG, M.S., PERRY, A.E. and CANTWELL, B. J. 1989 A general classification of three-dimensional flow patterns. *The Physics of Fluids* (to appear) (also SUDAAR 572).

LEWIS, G. S. 1989 An experimental investigation of low-speed non-premixed flames and buoyant jets using particle tracking. PhD. thesis Department of Mechanical Engineering Stanford University.

LEWIS, G. S., CANTWELL, B. J., VANDSBURGER, U. AND BOWMAN, C. T. 1988 An investigation of the interaction of a laminar non-premixed flame with an unsteady vortex. In *Proceedings of the 22nd Symposium (International) on Combustion*, The Combustion Institute pp. 515 - 522

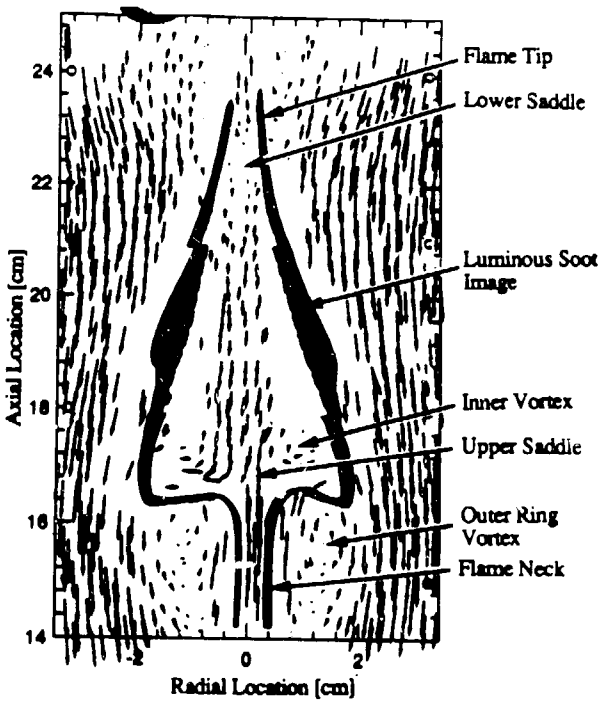

Figure 1 - Measured velocity vectors and soot envelope in a flickering methane-air diffusion flame.

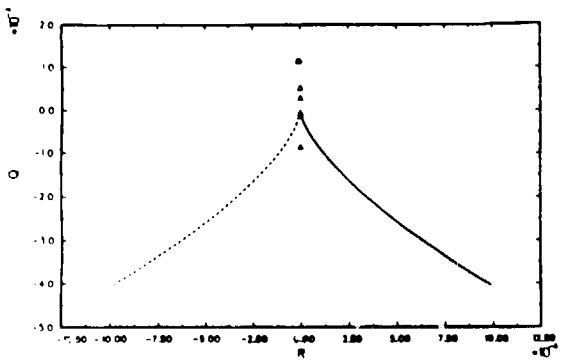

Figure 6 - Critical points of the fully developed wake in Q - R space.

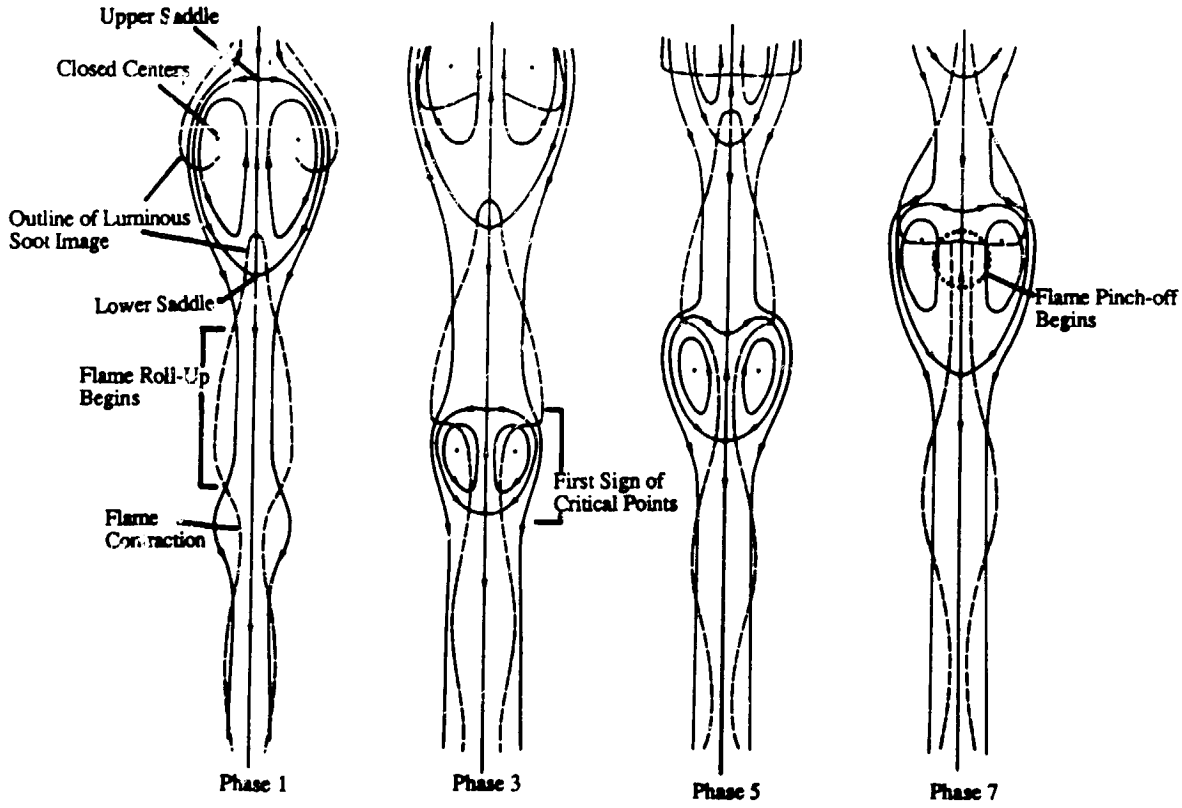

Figure 2 - Sequence of frames showing flame pinch-off.

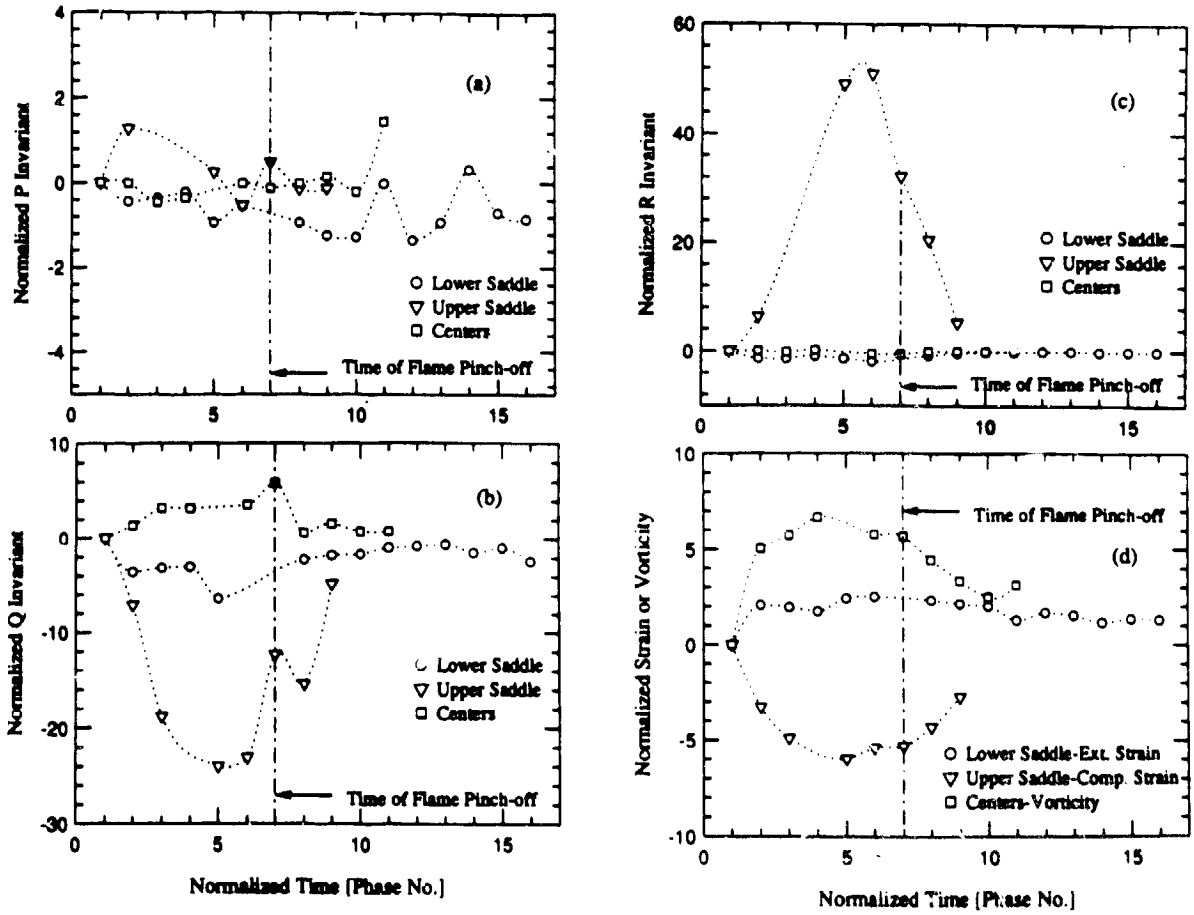

Figure 3 - Evolution of the invariants of the critical points in the flame; (a) P, (b) Q, (c) R, (d) strain or vorticity.

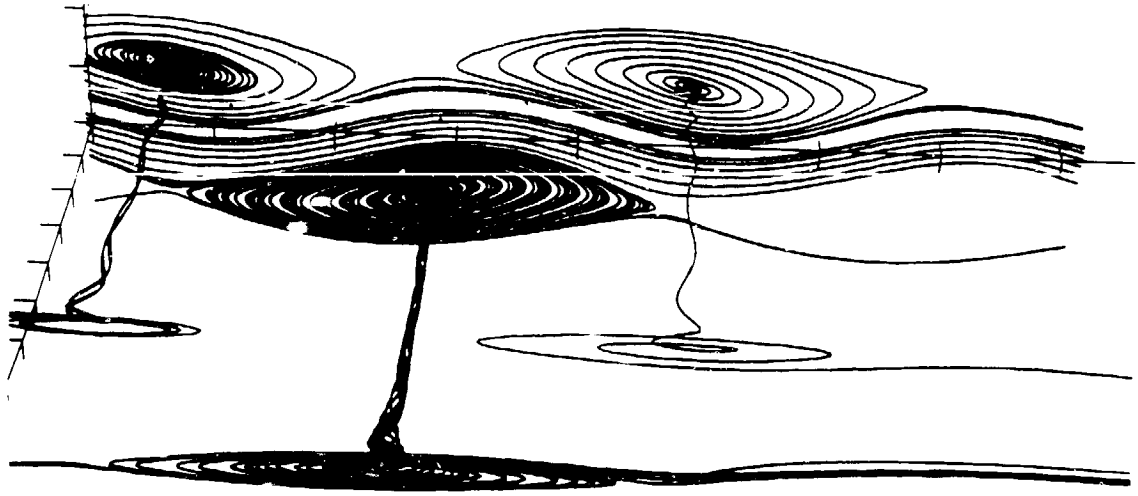

Figure 4 - Instantaneous streamlines in the wake shortly after the initiation of the motion.

Figure 5 - Two views of vortex lines in the fully developed wake at $t = 64$.

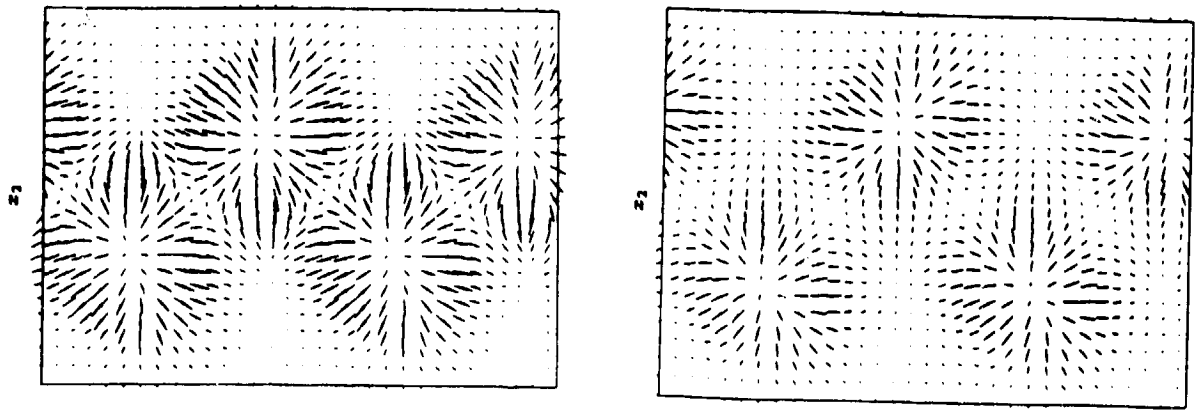

(a) (b)

Figure 7 - Pressure gradient vector field at $t = 59$; (a) in a plane through the maximum in streamwise vorticity, (b) in a plane with zero streamwise vorticity.